

Electronic Supplementary Information

What makes efficient circularly polarised luminescence in the condensed phase: Aggregation-induced circular dichroism and light emission

Jianzhao Liu,^{†,§} Huimin Su,[#] Luming Meng,[†] Yihua Zhao,[†] Chunmei Deng,[†] Jason C. Y. Ng,[†] Ping Lu,[†] Mahtab Faisal,[†] Jacky W. Y. Lam,^{†,§} Xuhui Huang,[†] Hongkai Wu,[†] Kam Sing Wong,^{*,#} and Ben Zhong Tang^{*,†,§,‡}

[†]Department of Chemistry, Institute for Advanced Study, Institute of Molecular Functional Materials, Division of Biomedical Engineering, State Key Laboratory of Molecular Neuroscience, The Hong Kong University of Science & Technology (HKUST), [#]Department of Physics, HKUST, Clear Water Bay, Kowloon, Hong Kong, China, [§]HKUST Fok Ying Tung Research Institute, Nansha, Guangzhou, China, and [‡]Department of Polymer Science and Engineering, Zhejiang University, Hangzhou 310027, China

* Corresponding authors. Phone: +852-2358-7375; Fax: +852-2358-1594; E-mails: phkswong@ust.hk; tangbenz@ust.hk

Table of Contents

Table S1. Crystal Data and Structure Refinement for 6 (CCDC 845739).	(S2)
Table S2. Fluorescence Decay Parameters of 1 in a Dilute Solution and Cast Thin Film.	(S3)
Table S3. Selected Reorganization Energies (λ) (>20 cm ⁻¹), Corresponding Huang-Rhys Factors (S) and Vibrational Frequencies (ω) of the First Excited State of TPS.	(S3)
Table S4. Calculated Energies of Different Packing Modes Shown in Figure 6 Based on HF/6-31(G) Level in Gaussian 03 Program.	(S4)
Figure S1. TGA thermogram of 1 recorded under nitrogen at a heating rate of 10 °C/min.	(S4)
Figure S2. Absorption spectra of 1 (A) in DCM/hexane mixtures with different concentrations and (B) dispersed in PMMA film with different weight fractions.	(S4)
Figure S3. Electron diffraction pattern of aggregates of 1 in DCM/hexane (1/9 v/v) mixture.	(S5)
Figure S4. Structural analysis of the intermolecular interactions in the energy-favored (a) longitudinal and (b) lateral pack models, which are extracted from D1 and D2 in Figure 6, respectively.	(S5)

Table S1. Crystal Data and Structure Refinement for 6 (CCDC 845739)

Empirical formula	C ₃₂ H ₂₈ N ₆ Si	
Formula weight	524.69	
Temperature	173.0 K	
Wavelength	1.5418 Å	
Crystal system	Orthorhombic	
Space group	Pbcn	
Unit cell dimensions	a = 20.8494(19) Å	α = 90 °
	b = 10.0000(7) Å	β = 90 °
	c = 13.5537(10) Å	γ = 90 °
Volume	2825.9(4) Å ³	
Z	4	
Density (calculated)	1.233 Mg/m ³	
Absorption coefficient	0.977 mm ⁻¹	
F(000)	1104	
Crystal size	0.35 × 0.32 × 0.02 mm ³	
Theta range for data collection	4.90 to 67.50 °	
Index ranges	-24 ≤ h ≤ 19, -11 ≤ k ≤ 11, -14 ≤ l ≤ 16	
Reflections collected	15833	
Independent reflections	2532 [R(int) = 0.0549]	
Completeness to theta = 66.50 °	99.6 %	
Absorption correction	Semi-empirical from equivalents	
Max. and min. transmission	1.00000 and 0.82112	
Refinement method	Full-matrix least-squares on F ²	
Data / restraints / parameters	2532 / 0 / 186	
Goodness-of-fit on F ²	1.031	
Final R indices [I > 2σ(I)]	R1 = 0.0413, wR2 = 0.1049	
R indices (all data)	R1 = 0.0588, wR2 = 0.1148	
Largest diff. peak and hole	0.174 and -0.244 e.Å ⁻³	

Table S2. Fluorescence Decay Parameters of 1 in a Dilute Solution and Cast Thin Film^a

	A ₁ (%)	A ₂ (%)	τ ₁ (ns)	τ ₂ (ns)	<τ> (ns)
solution	100	0	0.03		0.03
film	39	61	0.46	2.49	1.70

^a Fluorescence decay was fitted by a double-exponential function $I = A_1 e^{-t/\tau_1} + A_2 e^{-t/\tau_2}$ and the weighted lifetime $\langle \tau \rangle$ was calculated according to $\langle \tau \rangle = \frac{A_1 \tau_1 + A_2 \tau_2}{A_1 + A_2}$, where A and τ are the fractional amount and PL lifetime of the shorter (1)- and longer (2)-lived species, respectively.

Table S3. Selected Reorganization Energies (λ) (>20 cm⁻¹), Corresponding Huang-Rhys Factors (S) and Vibrational Frequencies (ω) of the First Excited State of TPS

mode	ω (cm ⁻¹)	S	λ (cm ⁻¹)
1	25.97	2.5055	65.07
2	27.12	9.9246	269.20
6	66.79	3.6736	245.36
7	74.79	0.8854	66.22
8	77.86	7.0610	549.76
11	118.08	6.9721	823.28
14	158.15	0.5171	81.78
16	175.30	0.5590	97.99
17	183.01	1.4544	266.17
20	213.05	0.3452	73.55
22	236.69	0.4599	108.86
33	433.56	0.1880	81.52
36	516.78	0.0593	30.66
38	570.00	0.0741	42.24
69	929.84	0.0396	36.77
73	950.86	0.1308	124.37
105	1246.96	0.3613	450.50
109	1318.63	0.0366	48.32
118	1394.84	0.1967	274.37
119	1415.76	0.3925	555.73
129	1520.66	0.0316	48.06
131	1531.60	0.0894	136.98
139	1652.29	0.0677	111.80

Table S4. Calculated Energies of Different Packing Modes Shown in Figure 6 Based on HF/6-31(G) Level in Gaussian 03 Program

Packing Modes	E (hartree)	ΔE (hartree)	ΔE (kJ/mol)
monomer	-4508.35880	0	0
D1	-9016.74784	-0.03025	-79.42
D2	-9016.73038	-0.01278	-33.55
D3	-9016.73024	-0.01264	-33.19
D4	-9016.72592	-0.00833	-21.84
T1	-18033.51868	-0.08350	-219.21
T2	-18033.51255	-0.07736	-203.12
T3	-18033.50846	-0.07328	-192.39

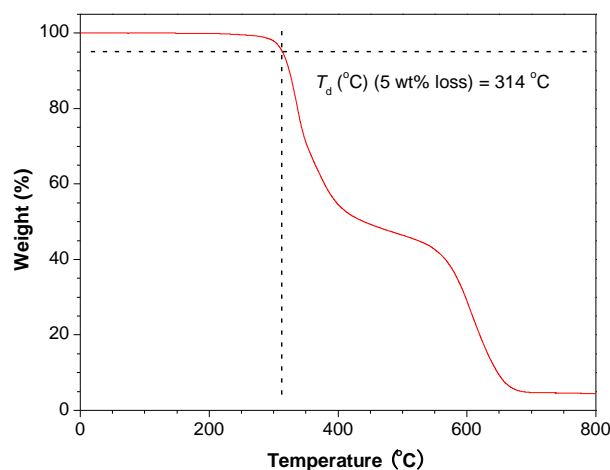


Figure S1. TGA thermogram of **1** recorded under nitrogen at a heating rate of 10 °C/min.

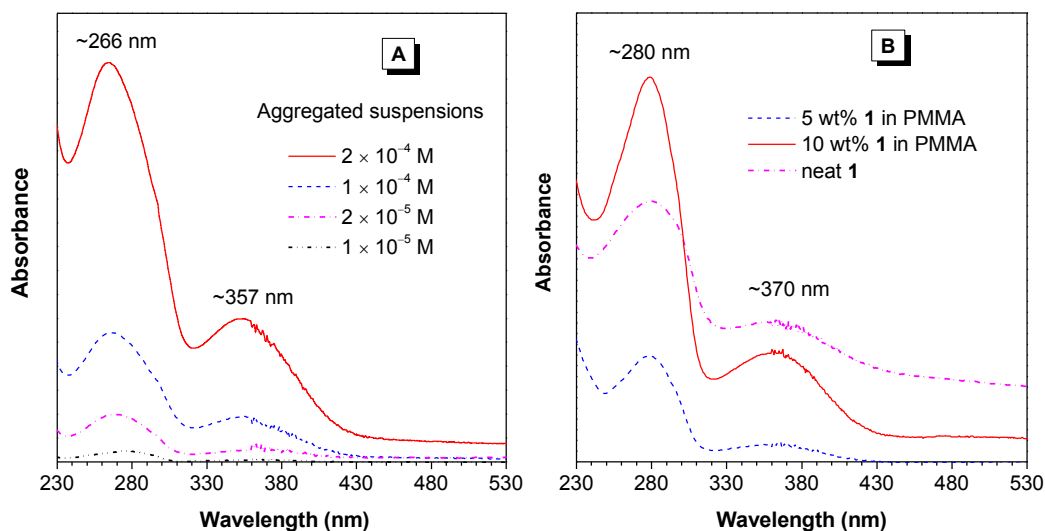


Figure S2. Absorption spectra of **1** (A) in DCM/hexane (1/9 v/v) mixtures with different concentrations and (B) dispersed in PMMA matrix with different weight fractions. Neat cast film of **1** in DCE is shown for comparison.

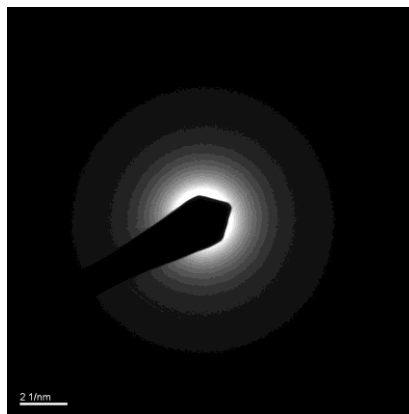


Figure S3. Electron diffraction pattern of aggregates of **1** in DCM/hexane (1/9 v/v) mixture.

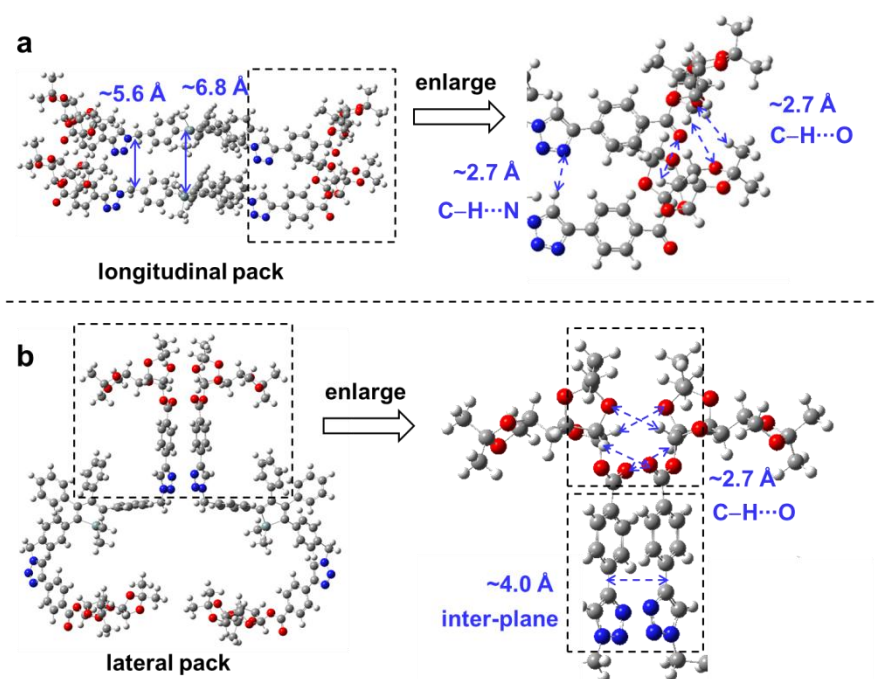


Figure S4. Structural analysis of the intermolecular interactions in the energy-favored (a) longitudinal and (b) lateral pack models, which are extracted from **D1** and **D2** in Figure 6, respectively.